Experimental Neurology 321 (2019) 113039

Contents lists available at ScienceDirect

Experimental Neurology

journal homepage: www.elsevier.com/locate/yexnr

Research Paper

Early TLR4 inhibition reduces hippocampal injury at puberty in a rat model of neonatal hypoxic-ischemic brain damage via regulation of neuroimmunity and synaptic plasticity

Zhen Tang[a], Shaowu Cheng[b], Yanyan Sun[a], Yunqiao Zhang[c], Xiying Xiang[d], Zhicui Ouyang[a], Xing Zhu[a], Bo Wang[d], Mingyan Hei[d,*]

[a] Department of Pediatrics, the Third Xiangya Hospital of Central South University, Changsha, Hunan 410013, China
[b] The Key Laboratory of Hunan Province for Integrated Traditional Chinese and Western Medicine on Prevention and Treatment of Cardio-Cerebral Diseases, Hunan University of Chinese Medicine, Changsha, Hunan 410208, China
[c] Neuropsychological Center, Sixth Affiliated Hospital, Kunming Medical University, Yunnan, 653100, China
[d] Neonatal Center, Beijing Children's Hospital, Capital Medical University, Beijing, 100045, China

ARTICLE INFO

Keywords:
Hypoxia-ischemia(HI)
Neuroprotection
Brain injuries
Hippocampus
Toll-like receptor 4
Rat model

ABSTRACT

Neonatal hypoxic-ischemic brain damage (HIBD) survivors present with long-term neurological disorders affecting their quality of life, and there remains a lack of effective treatment. Toll-like receptor 4 (TLR4) is widely distributed in nerve cells and its inhibition has a neuroprotective effect against brain injury. The present study aimed to evaluate the long-term neuroprotective effects of early inhibition of TLR4 during HIBD. Seven-day-old rat pups were subjected to left carotid artery ligation followed by 2 h of hypoxia (8.0% O_2). A single dose of TAK-242 (0.5 mg/kg), a TLR4-specific antagonist, was intraperitoneally injected half an hour prior to hypoxic ischemia (HI). The long-term effects of TAK-242 inhibition on the induced hippocampal injury were investigated by assessing behaviour at P28, and then using a variety of methods to exploring the mechanism, including immunofluorescence, Golgi silver staining, Western blotting and real-time polymerase chain reaction (RT-PCR). TAK-242 treatment significantly reduced the expression levels of TLR4 and its downstream signalling molecules in the ipsilateral lesion of the hippocampus 24 h after HIBD. The Morris water maze (MWM) test demonstrated that TAK-242 treatment reduced the loss of HI-induced learning and memory functions. Immunofluorescence experiments showed that TAK-242 administration attenuated HI-induced loss of neurons, prevented the activation of microglia and astrocytes, and increased the expression of the glutamate receptor subtype, *N*-methyl D-aspartate 2A (NR2A) in the ipsilateral hippocampus region. Golgi silver staining revealed that TAK-242 prevented an HI-induced decline in spine density in the ipsilateral hippocampus. Western blot and RT-PCR results indicated that the expression of NR2A protein and mRNA in the ipsilateral hippocampi of adolescent rats decreased after neonatal HIBD; early TAK-242 administration may reverse these effects. In conclusion, our findings indicate that early inhibition of TLR4 signalling may improve the long-term prognosis of neonatal HIBD. The mechanisms contributing to this improvement involve reductions in neuronal loss, a decrease in glial cell activation, and an improvement in synaptic plasticity.

1. Introduction

The prognosis of hypoxic-ischemic brain damage (HIBD) mainly depends on the severity of HIBD and the promptness of treatment (Lee et al., 2013; Glass et al., 2009). About a quarter of HIBD survivors worldwide suffer from long-term neurological disorders, such as epilepsy, cerebral palsy, blindness, and motor dysfunction every year, which places a heavy burden on the families of the afflicted, as well as society in general (Douglas-Escobar and Weiss, 2015; Eunson, 2015). The proportion of moderate HIBD with adverse outcomes reaches 32%, while almost all survivors of severe HIBD survivors have residual sequelae (Pin et al., 2009). Moreover, increasingly more HIBD survivors with no apparent disability still experience learning difficulties during childhood and adolescence as well as a series of neuropsychological problems, such as attention deficit and schizophrenia (Lindstrom et al., 2008; Hagberg et al., 2012). The limited treatment options available

* Corresponding author at: Neonatal Center, Beijing Children's Hospital, Capital Medical University, Nanlishi Road 56, Xicheng District, Beijing 100045, China.
E-mail address: heimingyan@bch.com.cn (M. Hei).

https://doi.org/10.1016/j.expneurol.2019.113039
Received 29 March 2019; Received in revised form 8 August 2019; Accepted 19 August 2019
Available online 20 August 2019
0014-4886/

also account for the poor prognosis of HIBD. Although mild hypothermia, the condition's only known effective treatment, can improve HIBD prognosis, it is difficult to implement within the optimal treatment window of 6 h after HI (Millar et al., 2017; Dixon et al., 2015; Natarajan et al., 2016). Clinical studies have also shown that although mild hypothermia administered to HIBD children at an early stage reduced acute death, cerebral palsy, blindness, and other serious adverse effects, school-age learning disabilities were not improved and intelligence quotient scores were also not significantly increased relative to a control group (Shankaran, 2012; Pappas et al., 2015). Therefore, improving the prognosis of HIBD, particularly reducing the long-term learning disabilities associated with HIBD, remains an important focus of current research efforts.

Increasing evidences show that crosstalk between the nervous and immune systems may affect the course of cognitive impairment after HIBD. The immune response, generated by cerebral HI, is an important cause of long-term cognitive impairment during development after early brain damage (Lai et al., 2017). Microglia are the most abundant resident innate immune cells in the brain. After brain injury, endogenous damage-associated molecular patterns (DAMPs) activate microglia, causing them to secrete inflammatory factors, such as tumour necrosis factor (TNF) and interleukin 1 beta (IL-1β), and initiate neuronal cell death pathways (Reemst et al., 2016; Li and Chen, 2016). Astrocytes with reactive hyperplasia inhibit acute injury amplification by accumulating to the lesion. However, overactivated astrocytes may release inflammatory cytokines and reduce neuronal function (Li et al., 2017; Verkhratsky and Nedergaard, 2018). These neuroimmune changes, activated primarily by glial cells, can persist long after the initial HI insult has been resolved, and may represent one of the mechanisms leading to long-term, poor neurological prognosis (Reemst et al., 2016). Changes in dendritic complexity and synaptic plasticity are closely related to long-term neurological dysfunction after brain injury. Decreased dendritic branch numbers and synaptic density can be found in neurodevelopmental disorders and ischemic brain injuries (Nobili et al., 2018; Sadigh-Eteghad et al., 2018). *N*-methyl-D-aspartic acid (NMDA) receptor is closely related to the development of synaptic function. The time of expression of the different NMDA receptor subunits in the developing hippocampus is indicative of the process of hippocampal synaptic development. However, NMDA receptors can also mediate neuronal cell death and synaptic-plasticity changes through increased binding of excitotoxic neurotransmitters during acute nerve injury. The application of NMDA antagonists to improve the long-term prognosis of brain injury, by regulating synaptic development, is controversial, especially in immature brains. (Zhang et al., 2014; Monyer et al., 1994; Millar et al., 2017).

Toll-like receptor 4 (TLR4) is the earliest discovered member of the mammalian TLRs and is widely expressed in neurons, as well as in glial cells, to help mediate neuroimmunity. The TLR4 signalling pathway activates various immune and endocrine factors that promote neuronal migration and synaptic maturation during brain development (Grasselli et al., 2018; Jones and Bouvier, 2014; Okun et al., 2012; Haydon and Nedergaard, 2014; Schepanski et al., 2018). When ischemia and traumatic brain injury occur, TLR4 signalling is activated via the myeloid differentiation primary response 88 (MyD88)-dependent or TIR-domain-containing adapter-inducing interferon-β (TRIF)-dependent pathways, inducing neuroinflammation and changes in synaptic plasticity; indeed, inhibiting the TLR4 pathway or knocking out the TLR4 gene significantly alleviates brain damage in animals (Ahmad et al., 2013; Wang et al., 2014; Brea et al., 2011). TAK-242 is an inhibitor selective for TLR4 and binds to the Toll/interleukin-1 receptor (TIR) domain of TLR4 and prevents its interaction with intracellular signalling molecules, thereby inhibiting the activation of downstream signalling pathways (Matsunaga et al., 2011). Animal experiments have demonstrated that TAK-242 has a protective effect on brain injury caused by acute cerebral ischemia-reperfusion, lipopolysaccharide exposure, or cerebral haemorrhage (Hua et al., 2015; Wang et al., 2013). However, it is not clear whether TAK-242 inhibition of TLR4 can improve the long-term prognosis of neonatal HIBD.

In this study, TAK-242 was used to inhibit the activity of TLR4 at the early stage of HI. The long-term effects of this inhibition on the induced hippocampal injury were investigated with behavioural, morphological, and molecular biological approaches to identify effective methods that may improve HIBD prognosis.

2. Materials and methods

2.1. Animals models

All animals were acquired from the Animal Management Centre of Central South University. The experimental design was approved by the Ethics Committee of the Third Xiangya Hospital of Central South University (NO:2016-S006). Every effort was made to minimise animal suffering and reduce the number of animals used in our experiments. Sprague–Dawley rats that were 16–18 days pregnant were kept separately in a barrier facility at a temperature of 25.0 ± 1.0 °C and with relative humidity of 60 ± 5% with food and water ad libitum under a 12 h light/12 h dark cycle. These conditions were designed to prevent exposing the animals to bright light or noise. Pups weighing 13–19 g were selected at P7. The pups were weaned and separated from their mother at P22. The HIBD model in neonatal rats was established according to the method detailed by Rice-Vannucci (Rice et al., 1981). Briefly, the animals were anaesthetised with isoflurane (4% induction, 2% maintenance) carried by O_2, and then the animals' left common carotid artery was located, the skin was cut, muscles and nerves were separated under the microscope, exposing the left common carotid artery. This artery was then cut in the middle after double ligation with a 5–0 suture. Lastly, the skin was sutured. The time under anaesthesia lasted no > 5 min. The pups were put into the dam after recovering from anaesthesia. One hour later, the pups were placed in a hypoxia chamber connected with an 8% O_2/92% N_2 mixture (1.5 L/min) in a constant-temperature water bath (37.0 °C). The oxygen concentration was maintained at 8.0 ± 0.1%. Anhydrous calcium chloride absorbed the animal's exhaled CO_2. After 2 h of hypoxia, the animals were placed back into the dam. In the control group, only the skin incision was performed to isolate and expose the common carotid artery; neither ligation, nor hypoxia, were administered to these animals.

Pups from each litter were randomly assigned to three groups: control, hypoxic- ischemia (HI), and HI + TAK-242 (TAK-242) (n = 35, Table 1). The sample size was calculated based on the literature reviewing and our previous experimental HIBD. Using a sample size calculator (power and sample size) with an alpha of 0.05 on a two-sided test, and a power of 0.8, the animal numbers n = 5/group was deemed to be sufficient for the experiments.TAK-242 (MedChemExpress USA) was dissolved in 1% dimethyl sulfoxide (DMSO) to a final concentration of 0.1 mg/mL, and a single intraperitoneal dose of 0.5 mg/kg was injected within the first half hour before HI (Yao et al., 2013). Both the control group and the HI group received intraperitoneal injections of saline containing the same volume and concentration of DMSO.

2.2. Morris water maze test

The Morris water maze (MWM) test was used to assess the spatial learning and memory of rats. It consisted of a labyrinth in a water pool (diameter, 160 cm; height, 50 cm) with a water temperature of 25.0 ± 1.0 °C; the water covered the platform to a depth of 1 cm. The pool was divided into four equivalent quadrants: north, west, south, and east. The platform was placed in a quadrant equidistant from the sidewall and the centre of the pool. At the start of the experiment, the rats were placed in a quadrant facing the wall and allowed to swim for 90 s or until the platform was found. If the animal found the platform, it could remain on it for 20 s. If the platform was not found, the animals were directed to the platform and allowed to remain on the platform for

Table 1
Study sample characteristics.

Group	Number	Male/Female	Death	Final number	Number of rats per test
Control	35	17/18	0	35	MWM (n = 10) H&E and IF (n = 5) Golgi silver staining (n = 5) Western blotting (24 h, n = 5;28 d, n = 5) RT-PCR (n = 5)
HI	35	20/15	3	32	MWM (n = 8, death 2) H&E and IF (n = 5)[a] Golgi silver staining (n = 5)[a] Western blotting (24 h, n = 5;28 d, n = 4, death 1) RT-PCR (n = 5)[a]
TAK-242	35	19/16	2	33	MWM (n = 9, death 1) H&E and IF (n = 5)[a] Golgi silver staining (n = 5) Western blotting (24 h, n = 5; 28 d, n = 5)[a] RT-PCR (n = 4, death 1)

Abbreviations: HI, hypoxia-ischemia; MWM, Morris Water Maze; H&E, haematoxylin-eosin; IF, immunofluorescence; RT-PCR, real-time polymerase chain reaction.
[a] Representatives include a case of hippocampal tissue loss.

20 s. A camera hanging above the maze and connected to a video tracking system, Panlab SMART V3.0 (Harvard Apparatus, USA), recorded the time taken and the distance covered by the rats to find the hidden platform. Beginning at P28, each rat was tested 4 times a day for 4 consecutive days. On the fifth day, the platform was removed for Probe Trials to record the percentage of the total time spent in the target quadrant, the percentage of the total distance covered in the target quadrant, and the number of times the rats crossed the location where the platform had previously been situated.

Tissue preparation.

All animals were euthanized after behavioural tests and their brains were preserved for tissue analysis. Except in rats, where the brains were to be used for Golgi silver staining, they were perfused sequentially from the heart with phosphate buffered saline (PBS) and 4% paraformaldehyde after being anaesthetized with pentobarbital (50 mg/kg). Brains were then removed and stored at −80 °C until further use. For biochemical analysis, animals were sacrificed by decapitation at the corresponding time point and the left-brain hemispheres were frozen on dry ice. All tissue samples were stored at −80 °C until used.

2.3. Golgi silver staining

Brain tissue samples were prepared and stained with the FD Rapid GolgiStain™ kit (FD NeuroTechnologies, Inc., USA) following the manufacturer's instructions. Brain tissue samples were trimmed to 1 cm^3 and then soaked in a mixture of 5 mL containing equal volumes of kit solution A and B, and incubated at room temperature for 2 weeks. The solution was replaced after the first 24 h. Subsequently, brain tissue samples were incubated in solution C at 4 °C for at least 72 h; the solution was also replaced after the first 24 h. Afterwards, 100 μm coronal slices were cut with a vibratome (Leica VT1000s, Germany) and fixed with 1% gelatine/0.1% chrome alum adhesives on the fragments containing solution C. The sections were then stained, dehydrated, and sealed with resin according to the manufacturer's instructions. A TissueFAXS PLUS microscope (TissueGnostics Imaging Solutions, Austria) was used to visualise neurons in the CA1 region of the hippocampus. Neurons were selected for analysis using the following criteria: (1) the cell body and dendrites were fully impregnated; (2) the cell was relatively isolated from surrounding neurons. The dendritic branches were measured using a 20× objective to count the bifurcations on each dendrite. First-order branches were dendritic segments prior to the first bifurcation from the soma, and branch orders gradually increased after each subsequent bifurcation. The number of first through sixth-order (and higher) branches were quantified to evaluate dendritic complexity (Candelaria-Cook and Hamilton, 2014). Imaging of the second- or third-order dendritic branches of hippocampal pyramidal neurons in the CA1 area was performed with a fixed *Z*-stack thickness using a 100× oil objective. The spine density (the number of spines per 10 μm) at mid-apical and basal compartments of the neurons was counted using ImageJ software (National Institutes of Health, USA). In each group, three neurons from the left hemispheres were randomly selected for blind observation and analysis.

2.4. Haematoxylin-eosin (H&E) and immunofluorescence staining

The brain tissues were thawed before slicing and then cut into 10 μm coronal sections using a cryostat slicing machine (Leica CM1510S, Germany). One slice every five slices was then selected for further analysis. Sections for H&E staining were first fixed, rinsed, and stained with haematoxylin and eosin. Sections were then dehydrated gradually using an alcohol gradient, adequately dried, sealed by neutral resin, and finally observed under a light microscope.

Sections for immunofluorescence testing were first fixed and then incubated at room temperature for 1 h in 5% bovine serum albumin containing 0.25% Triton X-100 solution. The specimens were then washed with PBS and incubated overnight with rabbit polyclonal anti-glial fibrillary acidic protein (GFAP; 1:400; Cell Signalling Technology, USA), mouse monoclonal anti-neuronal nuclei (NeuN; 1:500; Millipore, Germany), or rabbit polyclonal anti-ionised calcium-binding adaptor molecule 1 (Iba1; 1:500; Abcam). On the following day, the samples were washed once again with PBS and incubated for 1 h with corresponding Alexa Fluor 594-conjugated antibodies (1:200; Jackson ImmunoResearch Laboratories, Inc., USA) at room temperature. The nuclei were stained with 4′,6-diamidino-2-phenylindole (DAPI) and sealed with an anti-quenching agent. The expression of NMDA receptor subunits was evaluated similarly using the following antibodies: rabbit polyclonal anti-NR1 (1:200; Abcam), rabbit polyclonal anti-NR2A (1:200; Abcam), rabbit polyclonal anti-NR2B (1:200; Abcam), and Alexa Fluor 488-conjugated secondary antibody (1:200; Jackson ImmunoResearch Laboratories, Inc.). To identify glial cells in different states, a double immunofluorescence labelling method was used to determine the expression of IL-1β microglia (Iba-1/IL-1β) and astrocytes (GFAP/IL-1β). After incubation with the aforementioned secondary antibodies, the slices were washed with PBS and incubated overnight with mouse monoclonal anti-IL-1β antibody (1:100; Santa Cruz Biotechnology) at 4 °C. The sections were washed again with PBS the following day, and incubated with the corresponding Alexa Fluor 488-conjugated antibodies (1:200; Jackson ImmunoResearch Laboratories, Inc.) at room temperature for 1 h. The sections were observed and photographed under a fluorescence microscope (Olympus FluoviewTM FV1000, Olympus Corporation, Japan) using a 4× objective (for the whole hippocampus) or 20× objective (for the

hippocampal CA1, CA3, and DG regions). ImageJ software was used for quantitative analysis of immunoreactive sections. The number of NeuN-positive cells was counted along 250 μm length of medial CA1 pyramidal cell layer and the counts of three sections were averaged to provide a single value for each animal. The numbers of Iba-1-positive cells and GFAP-positive cells were counted and averaged in three different fields of the hippocampal CA1 region in three sections per rat, and data were expressed as cells/field.

2.5. Western blotting

The following antibodies were used for western blotting: rabbit polyclonal anti-TLR4 (1:1000; Abcam), rabbit polyclonal anti-MyD88 (1:1000; Abcam), rabbit polyclonal anti-TRIF (1:1000; Abcam), rabbit polyclonal anti-NR1 (1:2000; Abcam), rabbit polyclonal anti-NR2A (1:2000; Abcam), rabbit polyclonal anti-NR2B (1:2000; Abcam), and rabbit monoclonal anti-actin (1:5000; Abcam). After the ipsilateral hippocampal brain tissue was weighed, a mixture of RIPA lysis buffer (Beyotime Biotechnology, China) and phenylmethanesulfonyl fluoride (99:1; Sigma-Aldrich) was added to homogenise the tissue. The supernatant was collected after centrifugation at 4 °C and 12,000 ×*g* for 10 min. Protein concentrations were determined with a bicinchoninic acid assay. Samples (30 μg protein) were separated on 8–10% SDS-PAGE gels and transferred onto Polyvinylidene Fluoride membranes (Millipore). After blocking, the membranes were incubated with primary antibodies overnight at 4 °C. After routine washing with Tris Buffered Saline-Tween20 the next day, the goat anti-rabbit secondary antibody (1:3000; Abcam) were incubated at room temperature for 1 h with horseradish peroxidase-conjugated secondary antibodies. Enhanced chemiluminescence (ECL) (BioVision) was used for protein detection and the membranes were subsequently exposed on film. β-actin was used as a loading control. Quantity One™ 4.2.2 software (Bio-Rad) was used to analyse protein bands after scanning the film.

2.6. Real-time PCR

Total RNA was extracted using a TRIzol kit (Invitrogen, ThermoFisher Scientific, USA). Samples were homogenised with 1 mL TRIzol and RNA concentrations were determined by UV-spectrophotometry using a Nanodrop 2000 (ThermoFisher Scientific). A solution containing 2 μg of RNA was reverse-transcribed to complementary DNA (cDNA) using a RevertAid First Strand cDNA Synthesis Kit (Invitrogen, Thermo Fisher Scientific) according to the manufacturer's instructions. RT-PCR was performed in a 2.5 μL volume of cDNA using primers specific for *NR1*, *NR2A*, and *NR2B* (Table 2) and a master mix from the FastStart Universal SYBR Green Master (Rox) kit (Roche Life Science, USA), according to the manufacturer's instructions. The thermocycling conditions used were as follows: initial denaturation for 10 min at 95 °C and 40 cycles of denaturation at 95 °C for 15 s, annealing at 60 °C for 60 s, and extension at 72 °C for 10 s. All experiments were performed independently three times. Rat glyceraldehyde-3-phosphate dehydrogenase (GAPDH) was used as the internal housekeeping gene and the $2^{-\Delta\Delta Ct}$ method was employed to analyse changes in the target gene's expression.

Table 2
Primer sequences.

NR1	Forward 5′-CCACCTGAGTTTCCTTCGCAC-3′
	Reverse 5′-CCTTCTCTGCCTTGGACTCCC-3′
NR2A	Forward 5′-TAAACCTGGTGGCTGCTGAGG-3′
	Reverse 5′-GGCAATACCAGCAAGGTCCAG-3′
NR2B	Forward 5′-CTACGACACCTTCGTGGACCT-3′
	Reverse 5′-GTTGGCAAAGGAGCTCTCACC-3′
GAPDH	Forward 5′-ACTCTACCCACGGCAAGTTCA-3′
	Reverse 5′-CACGACATACTCAGCACCAGC-3′

NR: *N*-methyl-D-aspartic acid receptor; GAPDH: glyceraldehyde-3-phosphate dehydrogenase.

2.7. Statistical analysis

SPSS 20.0 software was used for data analysis. The data were presented as mean and standard deviation (mean ± SD). The statistical graphs were processed using Graph Pad Prism 5 (Graph Pad Software, San Diego, CA, USA) and Adobe Photoshop CS4 software (Adobe Systems Incorporated, San Jose, CA, USA). The results of the MWM tests and weight development assessments were performed using repeated measures ANOVA. The number of dendritic branches in the branch orders were analysed using two-way ANOVA. The other results were statistically analysed by one-way ANOVA. Bonferroni post hoc tests were performed for multiple comparisons. $P < .05$ was considered statistically significant.

3. Results

3.1. TAK-242 inhibits the activation of the TLR4 pathway in the rat hippocampus after HIBD

The expression levels of TLR4, MyD88, and TRIF were used to evaluate whether TAK-242 inhibits the activation of TLR4 pathways in the ipsilateral hippocampus of newborn rats after HIBD. The expression levels of TLR4, MyD88, and TRIF were higher in the HI group than in the control group at 24 h after HI ($P_{TLR4\ and\ MyD88} < 0.001$; $P_{TRIF} < 0.01$; Fig. 1); however, early injection of TAK-242 reduced TLR4, MyD88, and TRIF expression ($P < .01$; Fig. 1). These results show that TAK-242 can inhibit the activation of TLR4 pathways in the hippocampus of newborn rats after HIBD.

3.2. Early inhibition of TLR4 can alleviate HIBD-induced learning and memory impairments

The MWM test was used to evaluate the effects of TAK-242 on learning and memory ability after HIBD. There were no differences in weight or sex distribution between the three groups of newborn rats (n = 8–10; Fig. 2A, $F = 0.094$, $P = .911$; Fig. 2B, $P = 1.000$). Weight gain of the rats was not affected by HI (Fig. 2C; $F = 2.314$, $P = .121$). The hidden-platform test revealed statistically significant differences in escape latencies and distances covered (Fig. 2D and E; $F_{escape\ latency} = 17.366$; $F_{distance} = 14.226$; all $P < .001$). Further comparison showed that the swimming distances and the escape latencies were higher in the HI group than those in the control group (all $P < .05$); TAK-242 treatment reduced these HI-induced effects (all $P < .05$). Probe trials showed that the percentage of time spent in the target quadrant, the percentage of distance covered in the target quadrant, and the number of times the platform was crossed were significantly different among the groups (Fig. 2F, G and H; $F_{\%\ time} = 14.822$, $F_{\%\ distance} = 15.541$, $F_{crossing\ platform\ times} = 6.237$; all $P < .001$). Further comparison showed that the percentage of time spent in the target quadrant, the percentage of distance covered in the target quadrant, and the number of times the platform was crossed were all lower in the HI group than those in the control group (all $P < .05$). Although there was no significant difference in the number of times the platform was crossed between the TAK-242 and HI groups ($P > .05$), the percentage of time spent in the target quadrant and the percentage of distance covered in the target quadrant were higher in the TAK-242 group than those in the HI group (all $P < .05$). These experiments suggest that TAK-242 may alleviate the learning and memory impairments caused by HIBD in neonates.

3.3. Early administration of TAK-242 can reduce the loss of hippocampal neurons exhibited by rats in puberty after neonatal HIBD

H&E staining of coronal sections showed that neurons in the

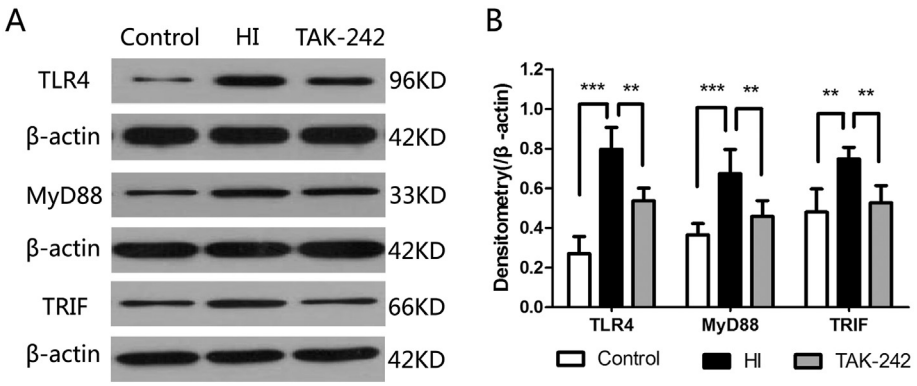

Fig. 1. TAK-242 can decelerate the activation of the TLR4 signalling pathway in the hippocampi of neonatal rats after HIBD. (A) Western blot analysis demonstrates levels of TLR4, MyD88, and TRIF in the hippocampi of rats at 24 h in control, HI, and TAK-242 groups. (B) Densitometry of the TLR4, MyD88, and TRIF bands are correlated with the β-actin band. $n = 5$/group.$^{**}P < .01$, $^{***}P < .001$.

hippocampal CA1, CA3, and dentate gyrus (DG) regions of rats were sparse and disorderly during puberty in rats exposed as neonates to HI. TAK-242 treatment prior to HI caused different degrees of improvement in the number and location of neurons (Fig. 3A). The number of NeuN-positive neurons in the CA1 area were lower in the HI group than that in the control group ($P < .001$; Fig. 3B and C). Treatment with TAK-242 prior to HI-induction increased the number of NeuN-positive neurons in the hippocampal CA1 area relative to the HI group ($P < .05$; Fig. 3B and C). These morphological changes suggest that TAK-242 has neuroprotective effects when administered before HIBD.

3.4. Early administration of TAK-242 can affect the activity of hippocampal glial cells of rats in puberty after neonatal HIBD

Although early administration of TAK-242 improved neuronal cell loss induced after HIBD, there were no differences in the number of

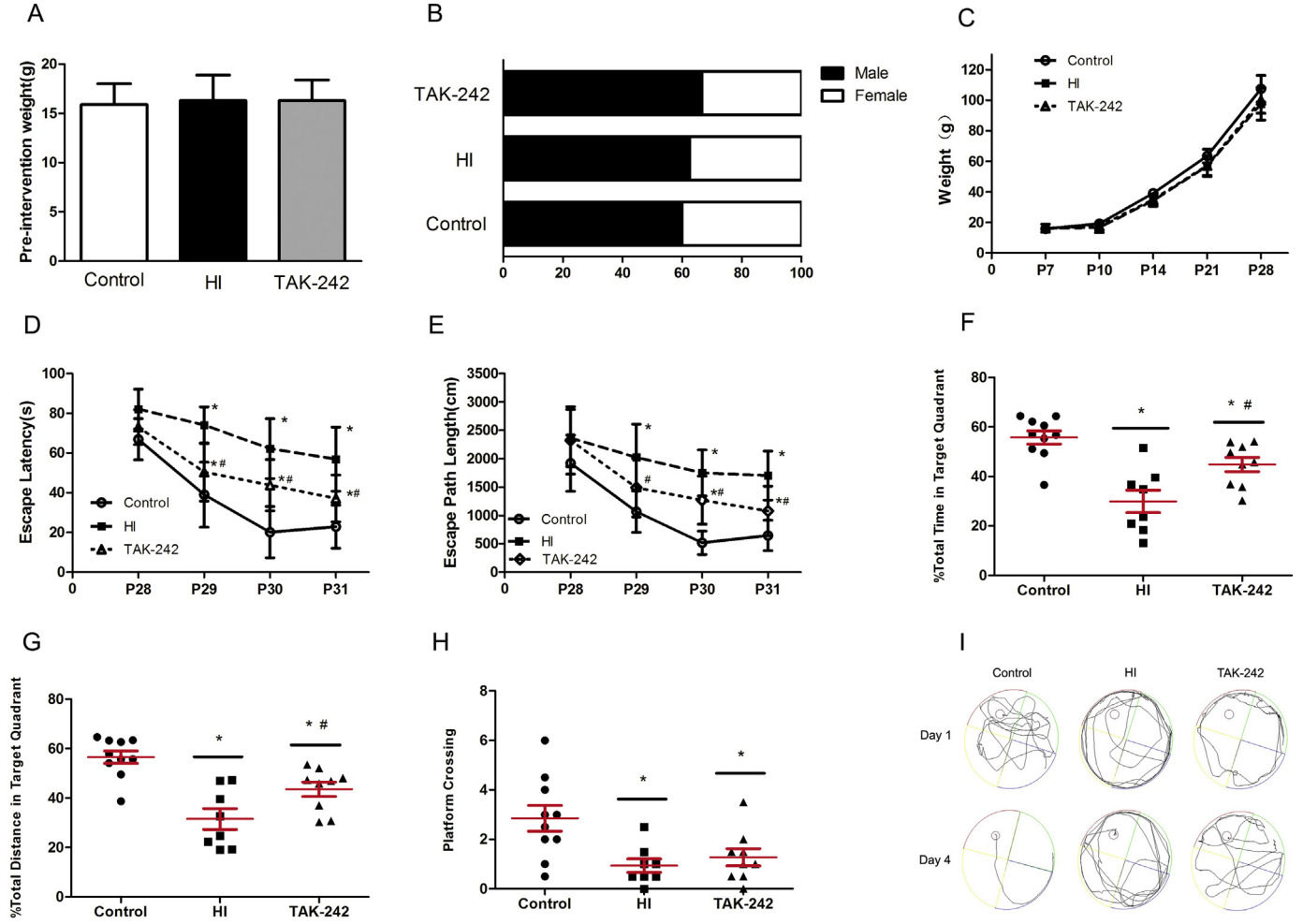

Fig. 2. Spatial memory deficits induced by neonatal HIBD are alleviated by the treatments of TAK-242. (A) Weight of each group before HIBD. (B) Sex distribution in each group. (C) Weight gain at each time point after HIBD. (D) Escape latency in the MWM plotted against training days. (E) Escape path length in the MWM plotted against training days. (F) The % total time spent in the target quadrant during the probe test of MWM. (G) The % total distance covered in the target quadrant during the probe test of MWM. (H) The number of platform crossings during a 90-s probe trial of the MWM test. (I) Representative swim paths of the rats obtained during trials 1 and 4. A repeated measures analysis of variance (ANOVA) was used with test day as the repeated measure and weight, latency, or distance swam, as the dependent variable. $n = 8$–10/group. *: significant different from the control group ($P < .05$) and #: significant difference from the HI group ($P < .05$).

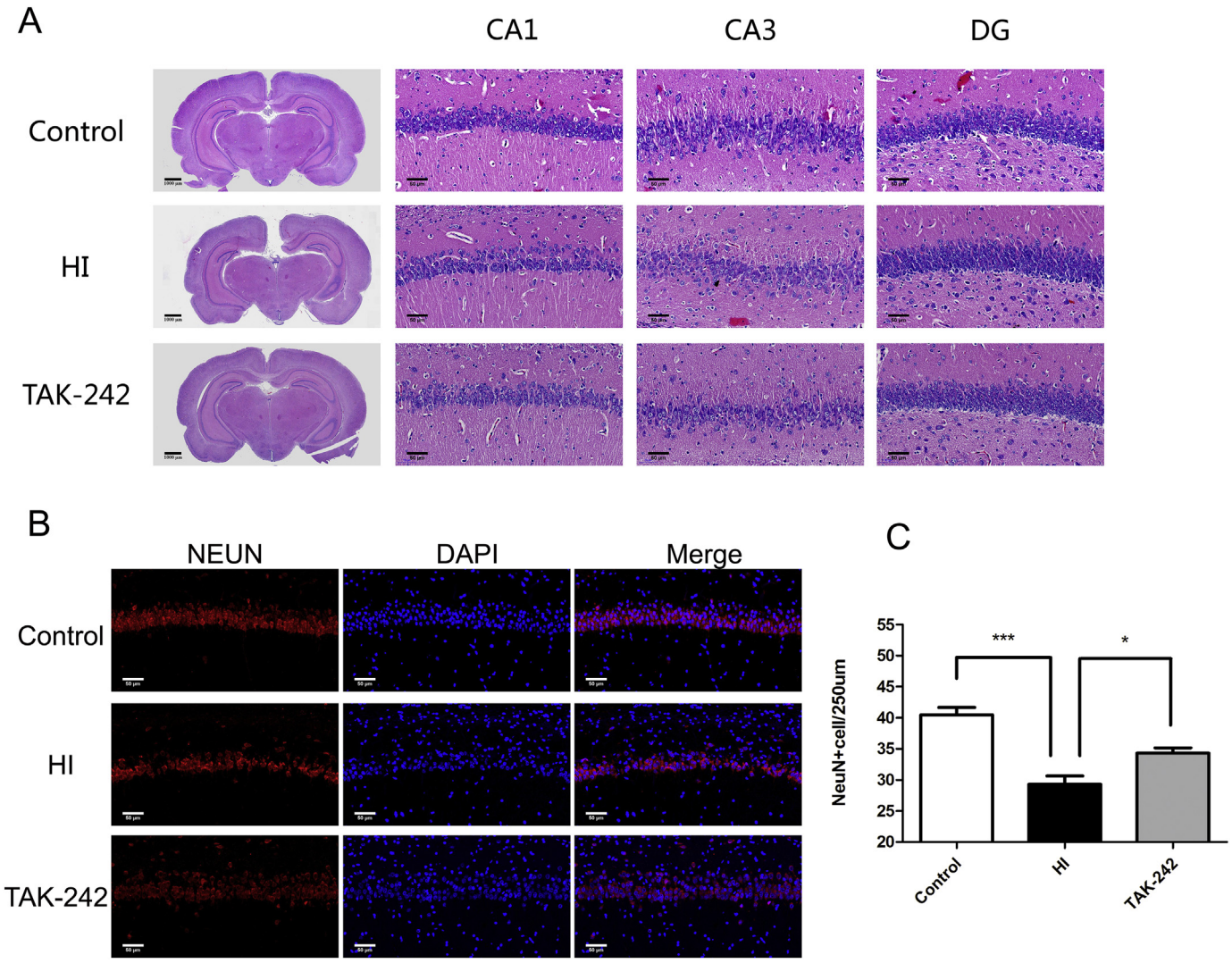

Fig. 3. TAK-242 treatment reduces hypoxia-ischemia induced brain damage in neonates. (A) Coronal sections stained with haematoxylin and eosin (H&E) from each group. The CA1, CA3, and DG regions were analysed. Whole-brain image: scale bar, 1000 μm; images of different brain regions: scale bar, 50 μm. (B) The brain slices of each group were labelled with NeuN in the CA1 region; scale bar, 50 μm. (C) The difference in the number of NeuN-positive cells in the CA1 region of each group. n = 4–5/group. $^{***}P < .001$; $^{*}P < .05$.

Iba1-positive microglia observed among the groups in the hippocampal CA1 region of rats during puberty (Fig. 4A and C; $P > .05$). By contrast, the number of GFAP-positive astrocytes in the hippocampal CA1 region of the HI group was significantly higher than that in the control group after neonatal HIBD (Fig. 4B and D; $P < .001$). Early administration of TAK-242 decreased the number of GFAP-positive astrocytes in the hippocampal CA1 region of the rats (Fig. 4B and D; $P < .05$). The secretion of inflammatory factors by glial cells was considered to be pro-inflammatory activation; we used IL-1β co-expression with glial cell markers as a marker of proinflammatory activation (Jaworska et al., 2017). Although there was no difference in the number of Iba-1 positive microglia among the experimental groups, IL-1β co-expression with Iba-1 positive microglia in the hippocampus CA1 region of the HI group was higher than that in the control group. Early administration of TAK-242 reduced Iba-1 positive microglia secretion of IL-1β (Fig. 5A). Concomitantly, IL-1β co-expression with GFAP-positive astrocytes in the HI group, also increased relative to the control group, and early TAK-242 treatment reduced the IL-1β co-expression with GFAP-positive astrocytes (Fig. 5B). These results suggest that TAK-242 may improve neuroimmune dysfunction in rats after HIBD.

3.5. Early administration of TAK-242 can improve the spine density of hippocampal neurons of rats during puberty after neonatal HIBD

Dendritic complexity and synaptic plasticity are important components of hippocampal neuron function (Lohmann and Kessels, 2014). In this study, Golgi silver staining was used to analyse the number of dendritic branches and spine density in each group to evaluate dendritic complexity and synaptic plasticity. Neurons in the hippocampal CA1 region of the rats were sparse and disorderly after HIBD (Fig. 6A). There were no significant group-branch order interactions ($F(10,234) = 1.107$; $P = .357$) and main effects ($F(2,234) = 0.672$; $P = .511$) for the number of dendritic branches at the base of CA1 neuron (Fig. 6B). To our surprise, two-way ANOVA between group and branch orders did not reveale a significant group-branch order interaction for the apical dendrites of CA1 neurons($F(10,234) = 1.770$; $P = .067$),but there were significant main effects of group ($F(2,244) = 4.193$; $P = .016$). Specifically, Bonferroni post hoc analyses revealed that HI decreased the number of dendritic branches at third-order and fourth-order branches compared to sham ($P < .05$), and TAK-242 did not alleviate this decrease ($P > .05$)(Fig. 6C). The density of second- or third-order dendritic branches at the basal and mid-apical compartments of the neurons decreased by varying degrees in the hippocampal

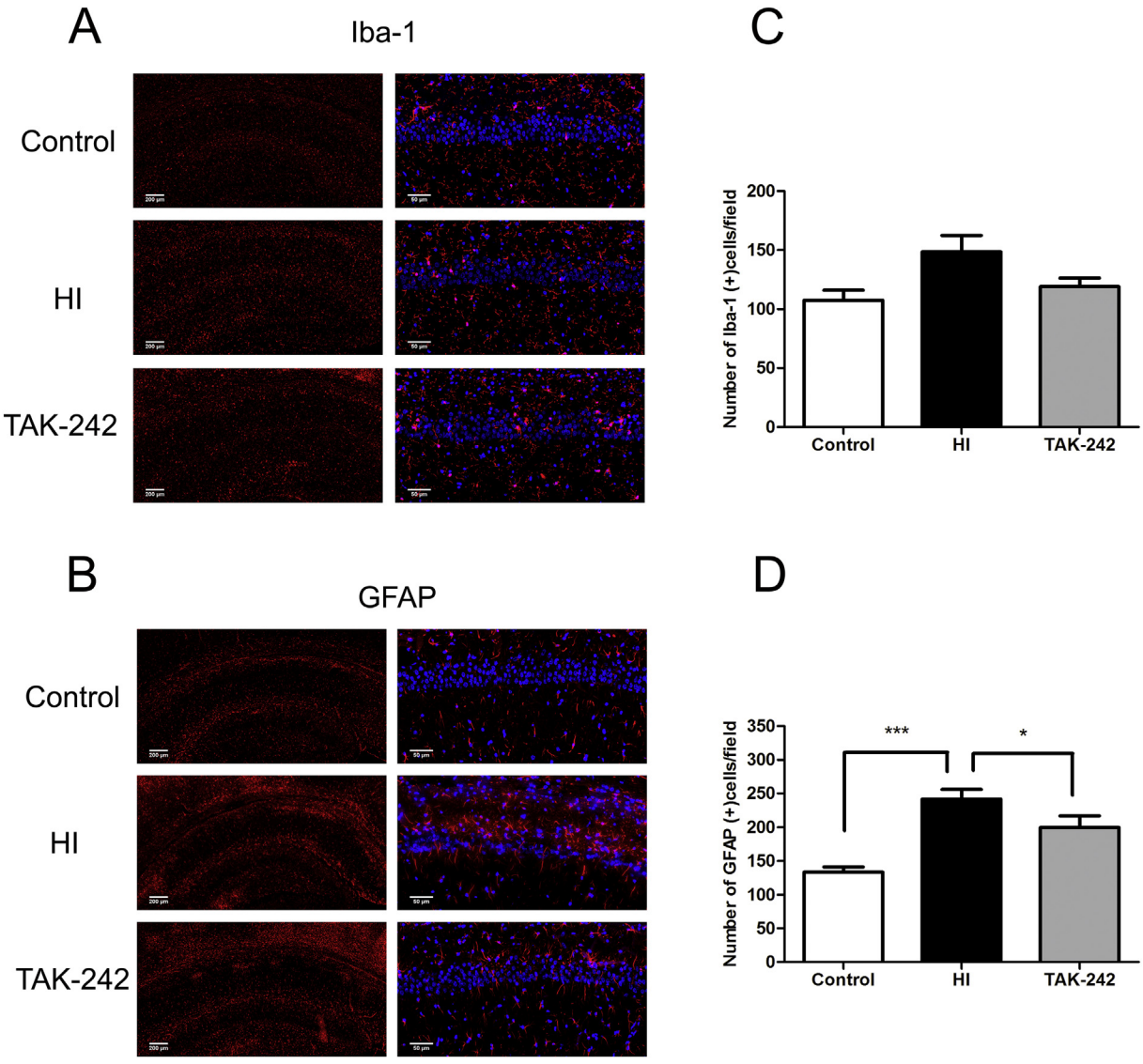

Fig. 4. TAK-242 treatment affects the distribution of glial cells after HIBD in neonates. (A) Positive expressions of Iba-1 used to represent the distribution of microglia in the hippocampus; Whole-hippocampus image: scale bar, 200 μm. Partial hippocampal image: scale bar, 50 μm. (B) Positive expression of GFAP used to represent the distribution of astrocytes in the hippocampus; Whole- hippocampus image: scale bar, 200 μm. Partial hippocampal image: scale bar, 50 μm. (C)The difference in the number of Iba-1-positive cells in the CA1 region of each group.(D)The difference in the number of GFAP-positive cells in the CA1 region of each group. $n = 4–5$/group. $^{***}P < .001$; *: $P < .05$.

CA1 region of the HI group relative to the control group (Fig. 6D, E, and F; all $P < .001$); Early TAK-242 treatment alleviated this decrease (Fig. 6D, E, and F; all $P < .05$).

3.6. Early administration of TAK-242 can improve the disturbance of NMDA expression in the hippocampus of rats during puberty after neonatal HIBD

The timely expression of NMDA receptors and their subunits is important for the maturation of neural functions, which is mainly manifested by its close correlation with the development of synapses (Lohmann and Kessels, 2014; Aow et al., 2015). Immunofluorescence showed that the expression of NR1 and NR2A decreased in the hippocampi of rats with HIBD, while the expression of NR2B increased; TAK-242 attenuated this change (Fig. 7). Western blot and RT-PCR also demonstrated that NR2A protein expression and *NR2A* mRNA levels in the hippocampi of rats with HIBD were significantly lower relative to the control group (Fig. 8A, C, F; all $P < .01$); NR1 and NR2B protein expression and *NR1* and *NR2B* mRNA levels were not significantly different between these two groups (Fig. 8A, B, D, E, G; all $P > .05$). TAK-242 treatment reduced NR2A protein expression and *NR2A* mRNA levels in the hippocampi of rats with HIBD (Fig. 8A, C, F; all < 0.05). However, there were no statistically significant differences between NR1 and NR2B protein, or mRNA levels, in the hippocampi of rats between the HI and TAK-242 groups (Fig. 8A, B, D, E, G; all $P > .05$).

4. Discussion

Impairment of hippocampal functions mainly manifests as a dysfunction in learning and memory. Neurogenesis in the adolescent hippocampus (in rats, 21–60 d; equivalent age in humans, 12–18 years) is four times higher than that in the adult hippocampus and is characterised by an increase in hippocampal volume and the number of granulosa cells. Puberty is the key period for the development of cognitive and signal integration functions and determines hippocampal function in adulthood (Spear, 2000; Curlik et al., 2014; He and Crews, 2007). Exposure to a variety of risk factors (including trauma, stress, and abuse) early in life may affect adolescent hippocampal functions

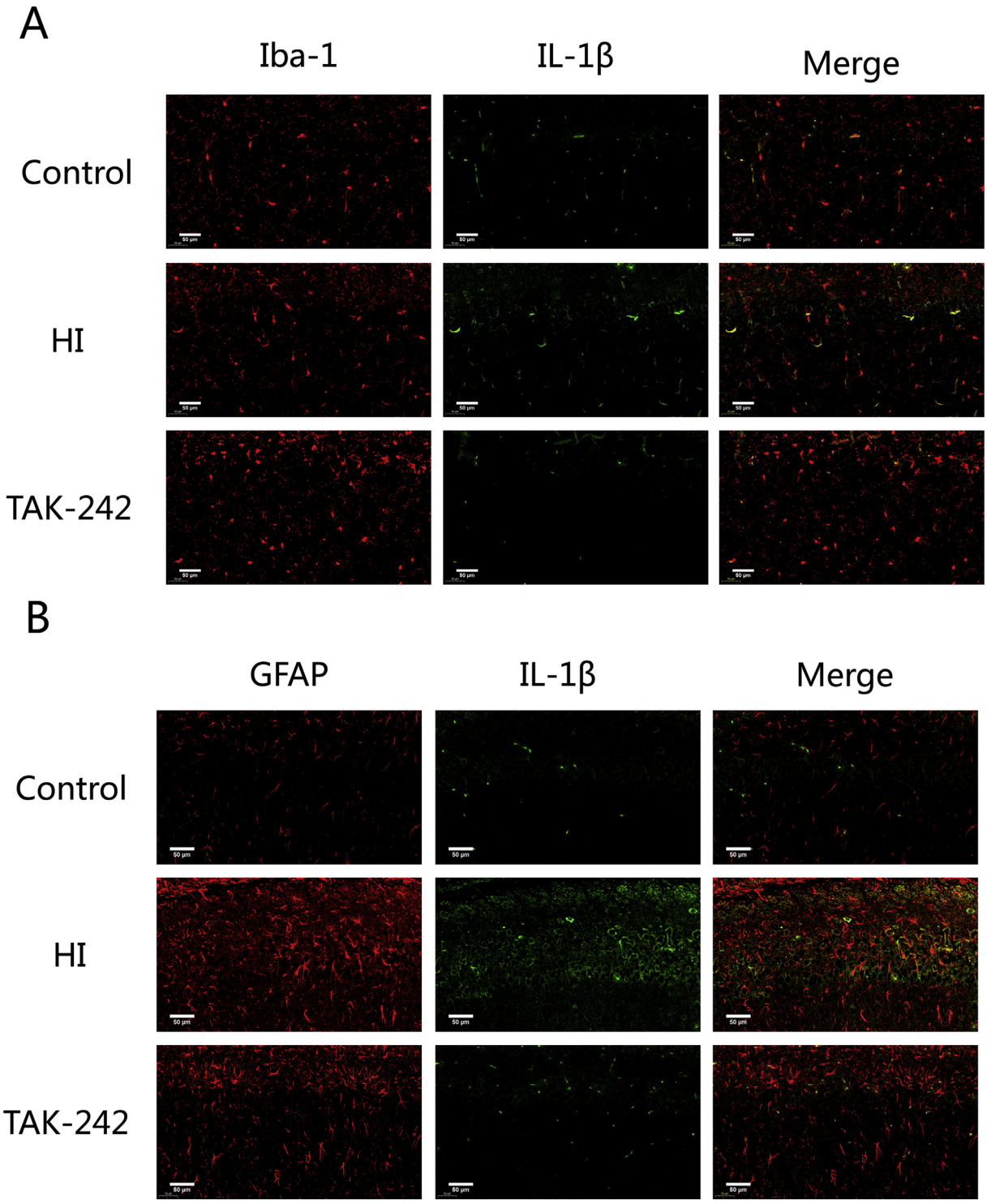

Fig. 5. TAK-242 decreases IL-1β expression in glia. (A) Brain sections from CA1 hippocampal regions were stained for Iba-1 immunoreactivity (red) and for IL-1β (green). (B) Brain sections from CA1 hippocampal regions were stained for GFAP immunoreactivity (red) and for IL-1β (green). Orange labelling indicates co-localisation. IL-1β immunofluorescence intensity of Iba-1/GFAP-positive cells were increased after HI and reduced after TAK-242 treatment; scale bar, 50 μm. n = 4–5/group. (For interpretation of the references to colour in this figure legend, the reader is referred to the web version of this article.)

and reduce quality of life as an adult (Kier et al., 1997; Insausti et al., 2010; Seress et al., 2001). Neonatal HIBD is a serious disease in the neonatal period as the hippocampus is a region especially vulnerable to hypoxic-ischemic effects. Clinical studies have confirmed that perinatal HIBD can lead to learning disabilities and memory impairments during childhood and adolescence, and its effects on quality of life can persist through adulthood (Douglas-Escobar and Weiss, 2015; Marlow et al., 2005; Odd et al., 2009). In this study, early treatment with the TLR4 inhibitor, TAK-242, improved the hippocampal function of pubertal rats after neonatal HIBD by alleviating neuronal loss and neuroimmunological effects as well as by promoting synaptic plasticity in the hippocampus.

After neonatal HI, hippocampal blood supply decreases and the mitochondria of hippocampal neurons fail within a short period. This

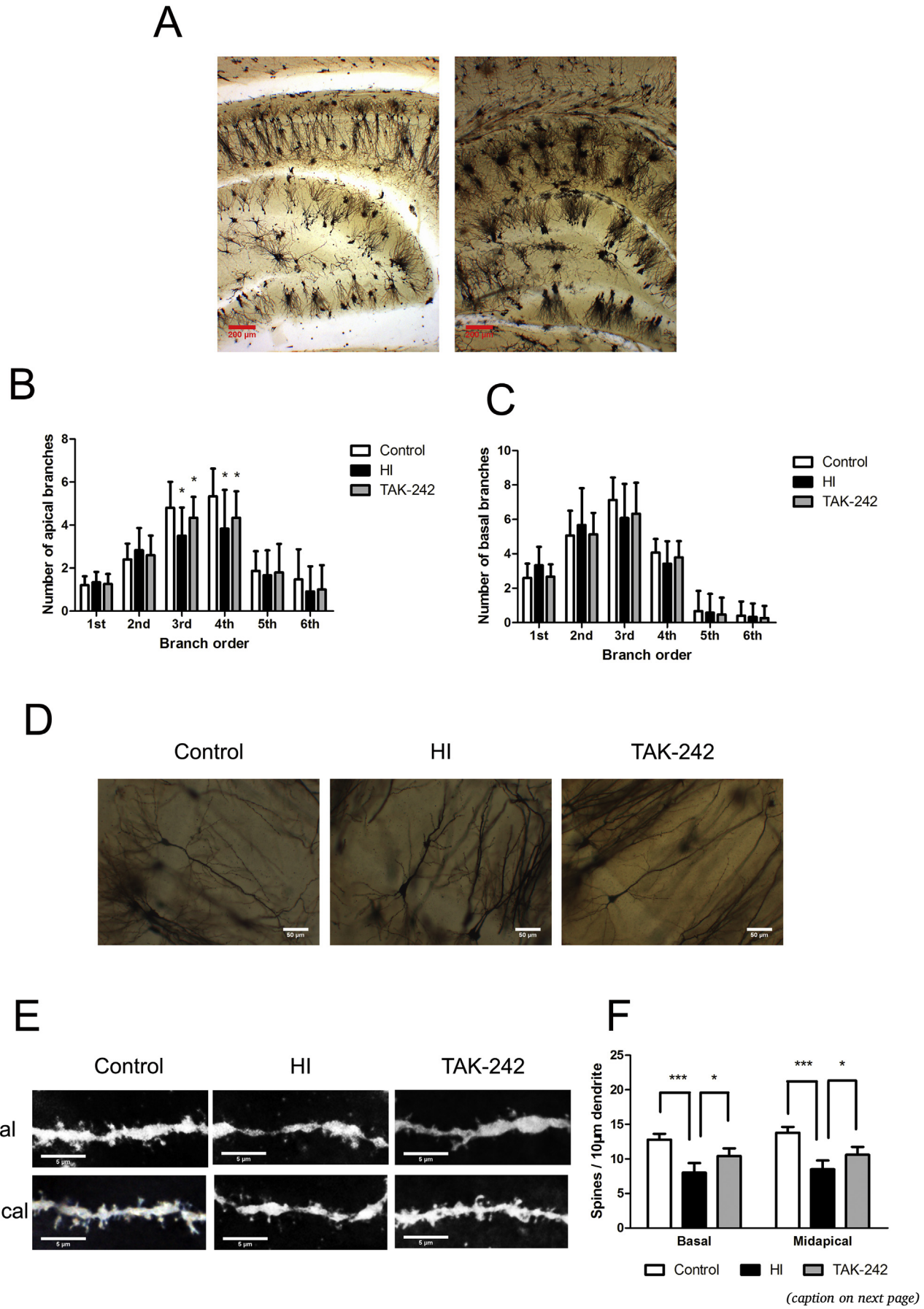

(caption on next page)

Fig. 6. TAK-242 treatment reduces HIBD-induced neurosynaptic deficiency. (A) Golgi silver staining shows the morphology of hippocampal neurons; scale bar, 200 μm. (B) (C) Mean number of apical and basal dendritic branches as a function of branch order for each group. *: significant difference from the control group ($P < .05$). (D) Morphology of basal and mid-apical neurons in each group after Golgi silver staining; scale bar, 50 μm. (E) Golgi silver staining of dendritic segments of mid-apical and basal surfaces of each group; scale, 5 μm. (F) The significant spine density deficits caused by HI were comparable in basal and mid-apical dendrites. TAK-242 may remedy spine density deficits. $n = 4–5$/group. $^{*}P < .05$, $^{***}P < .001$.

further result in acute cell death, the accumulation of neurotoxic substances, and neuroinflammation. These changes are not improved by blood supply recovery after reperfusion and the effects of neuronal cell death are sustained for a long period with accompanying changes in neuroimmunity (Titomanlio et al., 2015). Our study found that NeuN-positive neurons in the hippocampal CA1 region of neonatal rats decreased after HIBD compared to the control group. After HI, neuronal death occurs through various cell death mechanisms (including apoptosis, autophagy, and necrosis) that interact with one another, increasing the difficulty of attenuating cell death by addressing a specific mode of death. Eliminating neurotoxic substances and blocking neuroinflammation therefore, may constitute an effective strategy to alleviate neurological deficits induced by HIBD (Millar et al., 2017).

TLR4 is widely distributed on the surfaces of nerve cells and participates in the development and plasticity of neurons (Kang et al., 2014). However, animal experiments have shown that TLR4 expression is upregulated rapidly after brain injury; TLR4 binds to high mobility group protein B1 (HMGB1) and heat shock proteins (HSPs) and activates NF-κB-mediated neuronal death through the MyD88 and TRIF pathways (Ahmad et al., 2013; Wang et al., 2014; Brea et al., 2011; Lee et al., 2017; Allen and Barres, 2009). Nevertheless, the regulatory networks and duration of neuronal death in neonates with HIBD remain unclear. The present study found that early inhibition of the TLR4 pathway may improve hippocampal neuron loss during adolescence and confirmed that the inhibition of neuroinflammation may ameliorate neuronal death.

Acute and secondary brain injuries alter neuroimmunity leading to sustained injury in the later stages of brain injury. Microglia, derived from macrophages, play important roles mediating immunity in the central nervous system by regulating neurodevelopment and neuroplasticity, which are closely related to the development of hippocampal learning and memory functions (Cooper et al., 2015; Deierborg et al., 2010). When various injuries occur, overactivation of microglia through TLRs and mitogen-activated protein kinase (MAPK) pathways convert cells to an M1 phenotype, causing release of pro-inflammatory factors, such as IL-1β, IL-6, TNF-α, thereby yielding cytotoxic effects (Nagamoto-Combs et al., 2007). In experimental animal-brain trauma models and clinical observations of traumatic human brain injuries, microglial overactivation may last for months to years and is an important factor in the tertiary mechanism of brain injury (Ramlackhansingh et al., 2011; Sofroniew, 2009). Astrocytes are abundant cells in the central nervous system that originate from the neural lineage, providing a microenvironment for the survival of neurons, regulating formation and maturation of synapses, and releasing a series of factors to maintain the functional homeostasis of the central nervous system. Astrocytes are activated and aggregate into the lesion following acute brain injury to isolate necrotic neurons and play a protective role; however, if the excessive reactive astrocytes proliferation at the early stage of brain injury is not regulated, recovery of function in the central nervous system will be suppressed (Liddelow et al., 2017; He et al., 2019). The prolonged activation of astrocytes can inhibit axon regeneration and limit the transfer of toxic proteins by forming scars in the neuronal deletion area, leading to chronic nerve injury (Bruhn et al., 2000; Fellner et al., 2013). Our study showed that the number of Iba-1 positive microglia and the number of IL-1β co-expression with Iba-1-positive microglia were more in the hippocampi of adolescent rats after HIBD than those in the control group, although there was no statistically significant difference in the number of Iba-1 positive microglia between the HI and control groups. The number of GFAP-positive astrocytes and IL-1β co-expression in GFAP-positive astrocytes were significantly greater in the HI group than those in the control group, indicating that astrocyte proliferation and pro-inflammatory astrocytes participated in chronic brain injury after HI, as has been reported previously (He et al., 2019; Jaworska et al., 2017). In addition, the TLR4 pathway is an important pathway for glial cell activation; inhibition of TLR4 not only prevents the release of inflammatory mediators after acute brain injury but also regulates glial cell-mediated neuroinflammation and improves synaptic plasticity, which may be closely related to the improvement of age-related and Alzheimer's disease-induced chronic neurological impairment (Yao et al., 2013; Titomanlio et al., 2015; Shen et al., 2016; Malenka and Bear, 2004). Our study showed that the early inhibition of TLR4 may reduce the overactivation of hippocampal glial cells after HIBD, thus providing a new method for improving the long-term prognosis of neonatal HIBD.

Neuronal function is based on its dendritic morphology. Dendritic morphological parameters include dendritic length, number of dendritic branches, and dendritic complexity. Animal studies have shown that brain trauma and cerebral ischemia cause brain damage by changing dendritic morphology (Hoffman et al., 2017; Sadigh-Eteghad et al., 2018). This study also demonstrated that neonatal HI might also reduce the number of branches at partly orders (Third-order and Fourth-order branches) of apical dendrites in CA1 neurons.Unfortunately, TAK-242 treatment did not improve this decline. This suggests that early inhibition of TLR4 may not improve HI-mediated dendritic morphology, which requires further comprehensive studies to demonstrate. Changes in synaptic plasticity of hippocampal neurons are closely related to the learning and memory functions of the hippocampus, which are based on changes in synaptic density and protein structures on the synaptic membrane (Lohmann and Kessels, 2014). The critical period for synaptic development is considered 5–14 days after birth in rats. In human children, hippocampal synapses enter a rapid developmental stage during the perinatal period that lasts through the first 2 years of life and reach adult synaptic levels at about 5 years of age. In addition to an increase in the number of synapses, the level of development-related receptor proteins change during this critical period of development, providing conditions for the formation of long-term potentiation (LTP) and long-term depression (LTD), as well as learning and memory-related functions; however, the mechanisms and timing of LTP and LTD formation are not clearly understood at present (Nabavi et al., 2013). The NMDA receptor is an excitatory receptor on the synaptic membrane that may induce LTP and LTD to participate in hippocampal learning, memory, and cognitive development. However, activation of NMDA receptors through injury may also mediate neuronal death (Paoletti et al., 2013; Shipton and Paulsen, 2014). Although NR1 and NR2A expression increases after birth, NR2B expression levels reach their peak before birth (Lohmann and Kessels, 2014). The timing of this development is roughly the same for the development of synaptic plasticity, but the specific roles of NMDA receptors in the development of learning and memory functions remain to be elucidated. *NR2A*-gene knockout mice perform poorly in MWM tests, whereas NR2B inhibition does not affect long-term memory; short-term memory, however, is impaired in these animals (Sakimura et al., 1995; von Engelhardt et al., 2008; Cercato et al., 2016). In this study, Golgi silver staining showed that neonatal HIBD could reduce synaptic density in pubertal rats. Western blots and RT-PCRs demonstrated that NR2A expression in the hippocampus decreased, while the expression levels of NR2B and NR1 did not change significantly. These findings confirm that the NMDA

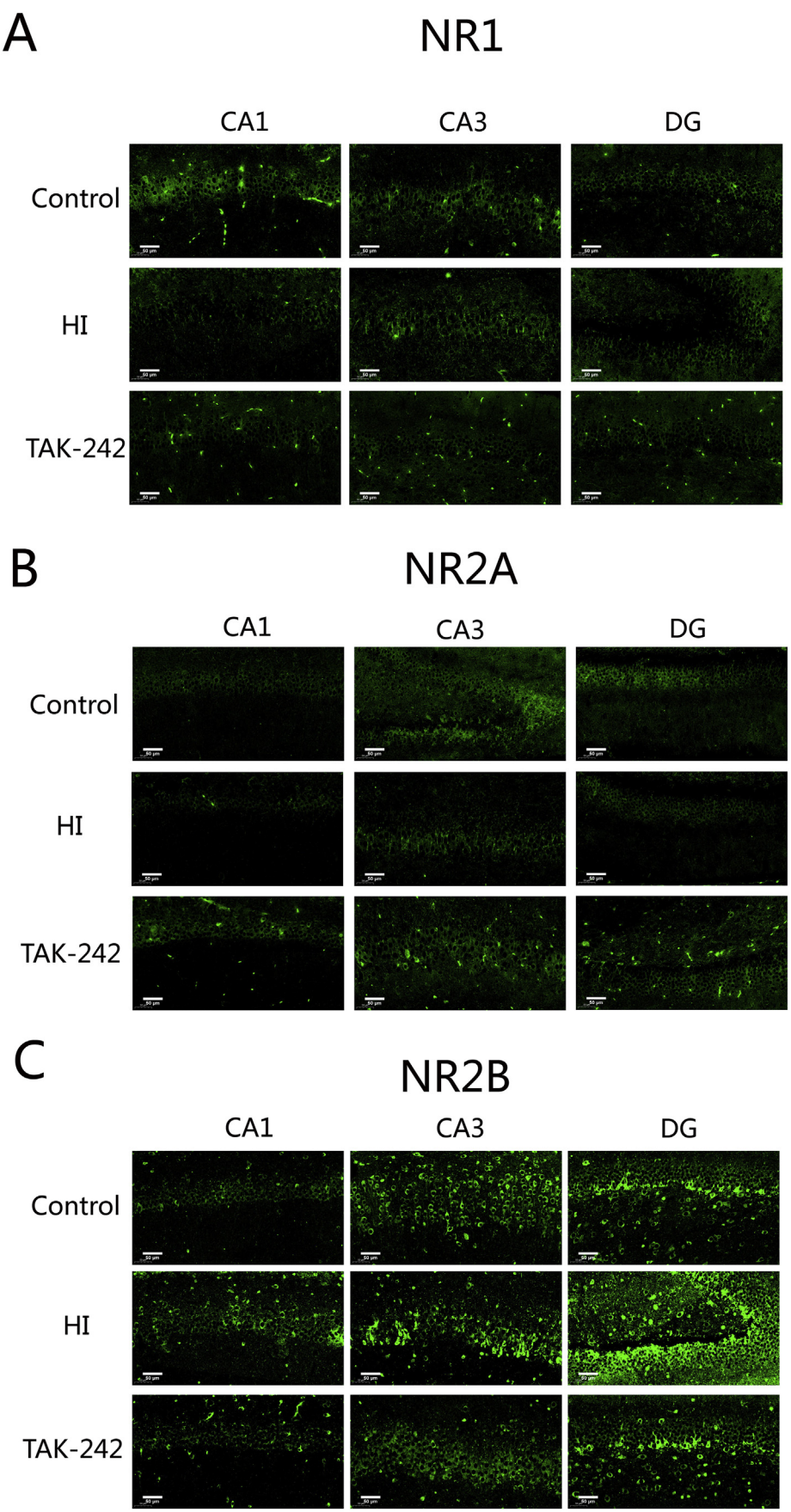

Fig. 7. TAK-242 treatment reduced the alteration of NMDA receptor expression in adolescent rats after HI. Immunofluorescence in hippocampi revealed the expression of the NMDA receptor subunits. (A) NR1 was expressed in the hippocampal CA1, CA3, and DG regions of each group. (B) NR2A was expressed in the hippocampal CA1, CA3, and DG regions of each group. (C) NR2B was expressed in the hippocampal CA1, CA3, and DG regions of each group; scale bar, 50 μm. n = 4–5/group.

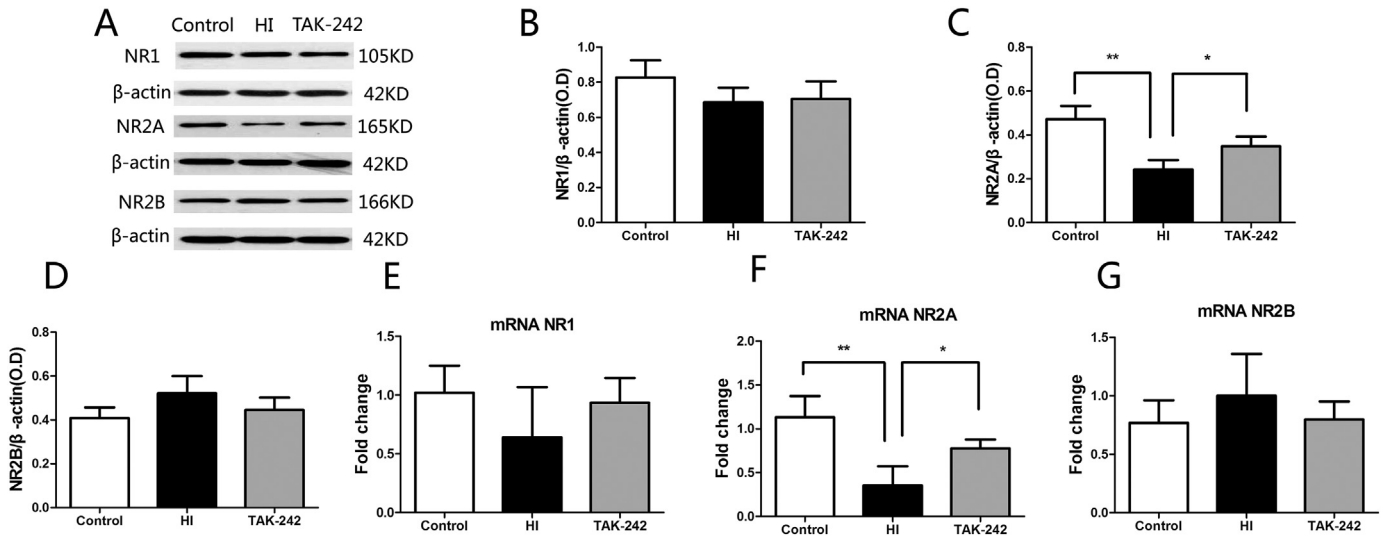

Fig. 8. TAK-242 treatment reduced the altered expression of NMDA receptors in adolescent rats after HI. Western blotting was used to detect expression of NMDA receptor subunits in the hippocampus. (A) NR1, NR2A, and NR2B expression in the hippocampi of each group were detected by Western blotting. (B–D) Bar graphs represent the statistical analysis of NR1, NR2A, and NR2B densitometric data from the experimental groups. Note the decrease of HI-induced reduction of NR2A after TAK-242 treatment at 21 days of recovery. (*E*-G) Bar graphs represent the statistical analysis of *NR1, NR2A,* and *NR2B* mRNA levels from the indicated experimental groups. Note the decrease of HI-induced reduction of *NR2A* mRNA after TAK-242 treatment at 21 days of recovery. $n = 4–5$/group.$^{*}P < .05$, $^{**}P < .01$.

receptor affects hippocampal function by participating in hippocampal plasticity. Early inhibition of TLR4 and the subsequent effect on neuroimmunity, were able to prevent the reduction in synaptic spine density and NR2A levels in adolescent rats, indicating that HI affects long-term neurological prognosis by altering neuroimmunity.

The findings of this study should be considered within the context of the study limitations. In this study, glial cell activity was not comprehensively evaluated despite its role in the regulation of synaptic plasticity. We also could not determine the specific mechanism of neuroimmune disorder on synaptic development after HIBD, including the possible overactivation of microglia and astrocytes contributing to the changes in synaptic density and the development of NMDA receptors. Changes in gene transcriptional levels and post-translational epigenetic modifications after HIBD may be the focus of our future research. Regardless of its limitation in scope, the present study found that early administration of TAK-242, a TLR4 inhibitor, reduced HI-induced adverse effects in the central nervous system, alleviated neuroinflammation induced by glial cells, and improved synaptic plasticity. This may provide a new method to improve the long-term prognosis in HIBD.

Funding

This work is supported by the National Natural Science Foundation of China (No. 81671505).

Declaration of competing interests

The authors declare that they have no conflicts of interest.

Acknowledgements

We are grateful for the substantial support of the central laboratory staff at the Third Xiangya Hospital of Central South University.

References

Ahmad, A., Crupi, R., Campolo, M., Genovese, T., Esposito, E., Cuzzocrea, S., 2013. Absence of TLR4 reduces neurovascular unit and secondary inflammatory process after traumatic brain injury in mice. PLoS One 8, e57208.
Allen, N.J., Barres, B.A., 2009. Neuroscience: glia – more than just brain glue. Nature 457, 675–677.
Aow, J., Dore, K., Malinow, R., 2015. Conformational signaling required for synaptic plasticity by the NMDA receptor complex. Proc. Natl. Acad. Sci. U. S. A. 112, 14711–14716.
Brea, D., Blanco, M., Ramos-Cabrer, P., Moldes, O., Arias, S., Perez-Mato, M., et al., 2011. Toll-like receptors 2 and 4 in ischemic stroke: outcome and therapeutic values. J. Cereb. Blood Flow Metab. 31, 1424–1431.
Bruhn, T., Levy, L.M., Nielsen, M., Christensen, T., Johansen, F.F., Diemer, N.H., 2000. Ischemia induced changes in expression of the astrocyte glutamate transporter GLT1 in hippocampus of the rat. Neurochem. Int. 37, 277–285.
Candelaria-Cook, F.T., Hamilton, D.A., 2014. Chronic cannabinoid agonist (WIN 55,212-2) exposure alters hippocampal dentate gyrus spine density in adult rats. Brain Res. 1542, 104–110.
Cercato, M.C., Vazquez, C.A., Kornisiuk, E., Aguirre, A.I., Colettis, N., Snitcofsky, M., et al., 2016. GluN1 and GluN2A NMDA receptor subunits increase in the hippocampus during memory consolidation in the rat. Front. Behav. Neurosci. 10, 242.
Cooper, J.M., Gadian, D.G., Jentschke, S., Goldman, A., Munoz, M., Pitts, G., et al., 2015. Neonatal hypoxia, hippocampal atrophy, and memory impairment: evidence of a causal sequence. Cereb. Cortex 25, 1469–1476.
Curlik, D.N., Difeo, G., Shors, T.J., 2014. Preparing for adulthood: thousands upon thousands of new cells are born in the hippocampus during puberty, and most survive with effortful learning. Front. Neurosci. 8, 70.
Deierborg, T., Roybon, L., Inacio, A.R., Pesic, J., Brundin, P., 2010. Brain injury activates microglia that induce neural stem cell proliferation ex vivo and promote differentiation of neurosphere-derived cells into neurons and oligodendrocytes. Neuroscience 171, 1386–1396.
Dixon, B.J., Reis, C., Ho, W.M., Tang, J., Zhang, J.H., 2015. Neuroprotective strategies after neonatal hypoxic ischemic encephalopathy. Int. J. Mol. Sci. 16, 22368–22401.
Douglas-Escobar, M., Weiss, M.D., 2015. Hypoxic-ischemic encephalopathy: a review for the clinician. JAMA Pediatr. 169, 397–403.
Eunson, P., 2015. The long-term health, social, and financial burden of hypoxic-ischaemic encephalopathy. Dev. Med. Child Neurol. 57 (Suppl. 3), 48–50.
Fellner, L., Irschick, R., Schanda, K., Reindl, M., Klimaschewski, L., Poewe, W., et al., 2013. Toll-like receptor 4 is required for alpha-synuclein dependent activation of microglia and astroglia. Glia 61, 349–360.
Glass, H.C., Glidden, D., Jeremy, R.J., Barkovich, A.J., Ferriero, D.M., Miller, S.P., 2009. Clinical neonatal seizures are independently associated with outcome in infants at risk for hypoxic-ischemic brain injury. J. Pediatr. 155, 318–323.
Grasselli, C., Ferrari, D., Zalfa, C., Soncini, M., Mazzoccoli, G., Facchini, F.A., et al., 2018. Toll-like receptor 4 modulation influences human neural stem cell proliferation and differentiation. Cell Death Dis. 9, 280.
Hagberg, H., Gressens, P., Mallard, C., 2012. Inflammation during fetal and neonatal life: implications for neurologic and neuropsychiatric disease in children and adults. Ann. Neurol. 71, 444–457.
Haydon, P.G., Nedergaard, M., 2014. How do astrocytes participate in neural plasticity? Cold Spring Harb. Perspect. Biol. 7, a20438.
He, J., Crews, F.T., 2007. Neurogenesis decreases during brain maturation from adolescence to adulthood. Pharmacol. Biochem. Behav. 86, 327–333.
He, M., Shi, X., Yang, M., Yang, T., Li, T., Chen, J., 2019. Mesenchymal stem cells-derived IL-6 activates AMPK/mTOR signaling to inhibit the proliferation of reactive astrocytes induced by hypoxic-ischemic brain damage. Exp. Neurol. 311, 15–32.
Hoffman, A.N., Paode, P.R., May, H.G., et al., 2017. Early and persistent dendritic hypertrophy in the basolateral amygdala following experimental diffuse traumatic brain

injury. J. Neurotrauma 34, 213–219.
Hua, F., Tang, H., Wang, J., Prunty, M.C., Hua, X., Sayeed, I., et al., 2015. TAK-242, an antagonist for Toll-like receptor 4, protects against acute cerebral ischemia/reperfusion injury in mice. J. Cereb. Blood Flow Metab. 35, 536–542.
Insausti, R., Cebada-Sanchez, S., Marcos, P., 2010. Postnatal development of the human hippocampal formation. Adv. Anat. Embryol. Cell Biol. 206, 1–86.
Jaworska, J., Ziemka-Nalecz, M., Sypecka, J., Zalewska, T., 2017. The potential neuroprotective role of a histone deacetylase inhibitor, sodium butyrate, after neonatal hypoxia-ischemia. J. Neuroinflammation 14, 34.
Jones, E.V., Bouvier, D.S., 2014. Astrocyte-secreted matricellular proteins in CNS remodelling during development and disease. Neural Plast. 2014, 321209.
Kang, R., Chen, R., Zhang, Q., Hou, W., Wu, S., Cao, L., et al., 2014. HMGB1 in health and disease. Mol. Asp. Med. 40, 1–116.
Kier, E.L., Kim, J.H., Fulbright, R.K., Bronen, R.A., 1997. Embryology of the human fetal hippocampus: MR imaging, anatomy, and histology. AJNR Am. J. Neuroradiol. 18, 525–532.
Lai, J., Rocha-Ferreira, E., Ek, C.J., Wang, X., Hagberg, H., Mallard, C., 2017. Immune responses in perinatal brain injury. Brain Behav. Immun. 63, 210–223.
Lee, A.C., Kozuki, N., Blencowe, H., Vos, T., Bahalim, A., Darmstadt, G.L., et al., 2013. Intrapartum-related neonatal encephalopathy incidence and impairment at regional and global levels for 2010 with trends from 1990. Pediatr. Res. 74 (Suppl. 1), 50–72.
Lee, B.S., Jung, E., Lee, Y., Chung, S.H., 2017. Hypothermia decreased the expression of heat shock proteins in neonatal rat model of hypoxic ischemic encephalopathy. Cell Stress Chaperones 22, 409–415.
Li, H., Chen, G., 2016. In vivo reprogramming for CNS repair: regenerating neurons from endogenous glial cells. Neuron 91, 728–738.
Li, B., Concepcion, K., Meng, X., Zhang, L., 2017. Brain-immune interactions in perinatal hypoxic-ischemic brain injury. Prog. Neurobiol. 159, 50–68.
Liddelow, S.A., Guttenplan, K.A., Clarke, L.E., Bennett, F.C., Bohlen, C.J., Schirmer, L., et al., 2017. Neurotoxic reactive astrocytes are induced by activated microglia. Nature 541, 481–487.
Lindstrom, K., Hallberg, B., Blennow, M., Wolff, K., Fernell, E., Westgren, M., 2008. Moderate neonatal encephalopathy: pre- and perinatal risk factors and long-term outcome. Acta Obstet. Gynecol. Scand. 87, 503–509.
Lohmann, C., Kessels, H.W., 2014. The developmental stages of synaptic plasticity. J. Physiol. 592, 13–31.
Malenka, R.C., Bear, M.F., 2004. LTP and LTD: an embarrassment of riches. Neuron 44, 5–21.
Marlow, N., Rose, A.S., Rands, C.E., Draper, E.S., 2005. Neuropsychological and educational problems at school age associated with neonatal encephalopathy. Arch. Dis. Child. Fetal Neonatal Ed. 90, F380–F387.
Matsunaga, N., Tsuchimori, N., Matsumoto, T., Ii, M., 2011. TAK-242 (resatorvid), a small-molecule inhibitor of Toll-like receptor (TLR) 4 signaling, binds selectively to TLR4 and interferes with interactions between TLR4 and its adaptor molecules. Mol. Pharmacol. 79, 34–41.
Millar, L.J., Shi, L., Hoerder-Suabedissen, A., Molnar, Z., 2017. Neonatal hypoxia ischaemia: mechanisms, models, and therapeutic challenges. Front. Cell. Neurosci. 11, 78.
Monyer, H., Burnashev, N., Laurie, D.J., Sakmann, B., Seeburg, P.H., 1994. Developmental and regional expression in the rat brain and functional properties of four NMDA receptors. Neuron 12, 529–540.
Nabavi, S., Kessels, H.W., Alfonso, S., Aow, J., Fox, R., Malinow, R., 2013. Metabotropic NMDA receptor function is required for NMDA receptor-dependent long-term depression. Proc. Natl. Acad. Sci. U. S. A. 110, 4027–4032.
Nagamoto-Combs, K., McNeal, D.W., Morecraft, R.J., Combs, C.K., 2007. Prolonged microgliosis in the rhesus monkey central nervous system after traumatic brain injury. J. Neurotrauma 24, 1719–1742.
Natarajan, G., Pappas, A., Shankaran, S., 2016. Outcomes in childhood following therapeutic hypothermia for neonatal hypoxic-ischemic encephalopathy (HIE). Semin. Perinatol. 40, 549–555.
Nobili, A., Krashia, P., Cordella, A., La Barbera, L., Dell'Acqua, M.C., Caruso, A., et al., 2018. Ambra1 shapes hippocampal inhibition/excitation balance: role in neurodevelopmental disorders. Mol. Neurobiol. 55, 7921–7940.
Odd, D.E., Lewis, G., Whitelaw, A., Gunnell, D., 2009. Resuscitation at birth and cognition at 8 years of age: a cohort study. Lancet 373, 1615–1622.
Okun, E., Barak, B., Saada-Madar, R., Rothman, S.M., Griffioen, K.J., Roberts, N., et al., 2012. Evidence for a developmental role for TLR4 in learning and memory. PLoS One 7, e47522.
Paoletti, P., Bellone, C., Zhou, Q., 2013. NMDA receptor subunit diversity: impact on receptor properties, synaptic plasticity and disease. Nat. Rev. Neurosci. 14, 383–400.
Pappas, A., Shankaran, S., McDonald, S.A., Vohr, B.R., Hintz, S.R., Ehrenkranz, R.A., et al., 2015. Cognitive outcomes after neonatal encephalopathy. Pediatrics 135, e624–e634.
Pin, T.W., Eldridge, B., Galea, M.P., 2009. A review of developmental outcomes of term infants with post-asphyxia neonatal encephalopathy. Eur. J. Paediatr. Neurol. 13, 224–234.
Ramlackhansingh, A.F., Brooks, D.J., Greenwood, R.J., Bose, S.K., Turkheimer, F.E., Kinnunen, K.M., et al., 2011. Inflammation after trauma: microglial activation and traumatic brain injury. Ann. Neurol. 70, 374–383.
Reemst, K., Noctor, S.C., Lucassen, P.J., Hol, E.M., 2016. The indispensable roles of microglia and astrocytes during brain development. Front. Hum. Neurosci. 10, 566.
Rice, J.R., Vannucci, R.C., Brierley, J.B., 1981. The influence of immaturity on hypoxic-ischemic brain damage in the rat. Ann. Neurol. 9, 131–141.
Sadigh-Eteghad, S., Geranmayeh, M.H., Majdi, A., Salehpour, F., Mahmoudi, J., Farhoudi, M., 2018. Intranasal cerebrolysin improves cognitive function and structural synaptic plasticity in photothrombotic mouse model of medial prefrontal cortex ischemia. Neuropeptides 71, 61–69.
Sakimura, K., Kutsuwada, T., Ito, I., Manabe, T., Takayama, C., Kushiya, E., et al., 1995. Reduced hippocampal LTP and spatial learning in mice lacking NMDA receptor epsilon 1 subunit. Nature 373, 151–155.
Schepanski, S., Buss, C., Hanganu-Opatz, I.L., Arck, P.C., 2018. Prenatal immune and endocrine modulators of offspring's brain development and cognitive functions later in life. Front. Immunol. 9, 2186.
Seress, L., Nelson, C., Luciana, M., 2001. Handbook of Developmental Cognitive Neuroscience. Morphological Changes of the Human Hippocampal Formation from Midgestation to Early Childhood Massachusetts Institute of Technology Press, Cambridge, MA, pp. 45–58.
Shankaran, S., 2012. Hypoxic-ischemic encephalopathy and novel strategies for neuroprotection. Clin. Perinatol. 39, 919–929.
Shen, Y., Qin, H., Chen, J., Mou, L., He, Y., Yan, Y., et al., 2016. Postnatal activation of TLR4 in astrocytes promotes excitatory synaptogenesis in hippocampal neurons. J. Cell Biol. 215, 719–734.
Shipton, O.A., Paulsen, O., 2014. GluN2A and GluN2B subunit-containing NMDA receptors in hippocampal plasticity. Philos. Trans. R. Soc. Lond. Ser. B Biol. Sci. 369, 20130163.
Sofroniew, M.V., 2009. Molecular dissection of reactive astrogliosis and glial scar formation. Trends Neurosci. 32, 638–647.
Spear, L.P., 2000. The adolescent brain and age-related behavioral manifestations. Neurosci. Biobehav. Rev. 24, 417–463.
Titomanlio, L., Fernandez-Lopez, D., Manganozzi, L., Moretti, R., Vexler, Z.S., Gressens, P., 2015. Pathophysiology and neuroprotection of global and focal perinatal brain injury: lessons from animal models. Pediatr. Neurol. 52, 566–584.
Verkhratsky, A., Nedergaard, M., 2018. Physiology of astroglia. Physiol. Rev. 98, 239–389.
von Engelhardt, J., Doganci, B., Jensen, V., Hvalby, O., Gongrich, C., Taylor, A., et al., 2008. Contribution of hippocampal and extra-hippocampal NR2B-containing NMDA receptors to performance on spatial learning tasks. Neuron 60, 846–860.
Wang, Y.C., Wang, P.F., Fang, H., Chen, J., Xiong, X.Y., Yang, Q.W., 2013. Toll-like receptor 4 antagonist attenuates intracerebral hemorrhage-induced brain injury. Stroke 44, 2545–2552.
Wang, Y., Ge, P., Yang, L., Wu, C., Zha, H., Luo, T., et al., 2014. Protection of ischemic post conditioning against transient focal ischemia-induced brain damage is associated with inhibition of neuroinflammation via modulation of TLR2 and TLR4 pathways. J. Neuroinflammation 11, 15.
Yao, L., Kan, E.M., Lu, J., Hao, A., Dheen, S.T., Kaur, C., et al., 2013. Toll-like receptor 4 mediates microglial activation and production of inflammatory mediators in neonatal rat brain following hypoxia: role of TLR4 in hypoxic microglia. J. Neuroinflammation 10, 23.
Zhang, X.Y., Ji, F., Wang, N., Chen, L.L., Tian, T., Lu, W., 2014. Glycine induces bidirectional modifications in N-methyl-D-aspartate receptor-mediated synaptic responses in hippocampal CA1 neurons. J. Biol. Chem. 289, 31200–31211.